2012

Molecular mechanisms used by chaperones to reduce the toxicity of aberrant protein oligomers

Benedetta Mannini
University of Florence

Roberta Cascella
University of Florence

Mariagiola Zampagni
University of Florence

Maria van Waarde-Verhagen
University of Groningen

Sarah Meehan
University of Cambridge

See next page for additional authors

Molecular mechanisms used by chaperones to reduce the toxicity of aberrant protein oligomers

Abstract

Chaperones are the primary regulators of the proteostasis network and are known to facilitate protein folding, inhibit protein aggregation, and promote disaggregation and clearance of misfolded aggregates inside cells. We have tested the effects of five chaperones on the toxicity of misfolded oligomers preformed from three different proteins added extracellularly to cultured cells. All the chaperones were found to decrease oligomer toxicity significantly, even at very low chaperone/protein molar ratios, provided that they were added extracellularly rather than being overexpressed in the cytosol. Infrared spectroscopy and site-directed labeling experiments using pyrene ruled out structural reorganizations within the discrete oligomers. Rather, confocal microscopy, SDS-PAGE, and intrinsic fluorescence measurements indicated tight binding between oligomers and chaperones. Moreover, atomic force microscopy imaging indicated that larger assemblies of oligomers are formed in the presence of the chaperones. This suggests that the chaperones bind to the oligomers and promote their assembly into larger species, with consequent shielding of the reactive surfaces and a decrease in their diffusional mobility. Overall, the data indicate a generic ability of chaperones to neutralize extracellular misfolded oligomers efficiently and reveal that further assembly of protein oligomers into larger species can be an effective strategy to neutralize such extracellular species.

Keywords

Publication Details

Authors

Benedetta Mannini, Roberta Cascella, Mariagiola Zampagni, Maria van Waarde-Verhagen, Sarah Meehan, Cintia Roodveldt, Silvia Campioni, Matilde Boninsegna, Amanda Penco, Annalisa Relini, Harm H. Kampinga, Christopher M. Dobson, Mark R. Wilson, Cristina Cecchi, and Fabrizio Chiti

Molecular chaperones reduce the toxicity of aberrant protein oligomers: molecular insight into the mechanism

Running title: Chaperones neutralize toxic protein oligomers

Benedetta Mannini°[1], Roberta Cascella°[1], Mariagioia Zampagni[1], Maria A.W.H. van Waarde-Verhagen[2], Sarah Meehan[3], Cintia Roodveldt[4], Silvia Campioni[5], Matilde Boninsegna[1], Amanda Penco[6], Annalisa Relini[6], Harm H. Kampinga[2], Christopher M. Dobson[3], Mark R. Wilson[7], Cristina Cecchi[1], Fabrizio Chiti*[1]

[1] *Department of Biochemical Sciences, University of Florence, V.le GB Morgagni 50, 50134 Florence, Italy*

[2] *Department of Cell Biology, University Medical Center Groningen, Hanzeplein 1, 9713 AV Groningen, The Netherlands*

[3] *Department of Chemistry, University of Cambridge, Lensfield Road, Cambridge, CB2 1EW Cambridge, United Kingdom*

[4] *CABIMER-Andalusian Center for Molecular Biology and Regenerative Medicine, CSIC-University of Seville-UPO-Junta de Andalucía, Americo Vespucio Ave,Parque Científico y Tecnológico Cartuja 93, 41092 Seville, Spain*

[5] *Department of Chemistry and Applied Biosciences, Eidgenössische Technische Hochschule Zürich, HCI G 313 Wolfgang-Pauli-Strasse 10 CH-8093 Zurich, Switzerland*

[6] *Department of Physics, University of Genoa, v. Dodecaneso 33, 16146, Genoa, Italy*

[7] *School of Biological Sciences, University of Wollongong, Wollongong NSW, 2522 Australia*

° These authors contributed equally to the work

* To whom correspondence should be addressed. E-mail: fabrizio.chiti@unifi.it

1

Abstract

Chaperones are the primary regulators of the proteostasis network and are known to facilitate protein folding, inhibit protein aggregation and promote disaggregation and clearance of misfolded aggregates inside cells. We have tested the effects of five chaperones on the toxicity of misfolded oligomers preformed from three different proteins added extracellularly to cultured cells. All the chaperones were found to decrease significantly oligomer toxicity even at very low chaperone/protein molar ratios, provided that they were added extracellularly rather than being overexpressed in the cytosol. Infrared spectroscopy and site-directed labelling experiments using pyrene ruled out structural reorganizations within the discrete oligomers. Rather, confocal microscopy, SDS-PAGE and intrinsic fluorescence measurements indicated tight binding between oligomers and chaperones. Moreover, AFM imaging indicated that larger assemblies of oligomers are formed in the presence of the chaperones. This suggests that the chaperones bind to the oligomers and promote their assembly into larger species, with consequent shielding of the reactive surfaces and a decrease in their diffusional mobility. Overall, the data indicate a generic ability of chaperones to neutralize efficiently extracellular misfolded oligomers and reveal that further assembly of protein oligomers into larger species can be an effective strategy to neutralize such extracellular species.

Introduction

\body The ability of living systems to maintain their peptides and proteins in soluble and functional states is the result of evolutionary selection of the physicochemical and conformational characteristics of these macromolecules (1) and owing to an array of biological mechanisms that together act to ensure proteostasis (2). Failures of the protective and regulatory mechanisms can result in a wide variety of pathological conditions, including those associated with the accumulation of protein aggregates, both in the cytosol and in the extracellular space (3,4). Molecular chaperones are proteins that play a central role in the avoidance of protein misfolding and aggregation (5-8). Most known chaperones are intracellular (7,8), but some of them are secreted and are collectively referred to as extracellular chaperones (9). Chaperones are known to have a range of different functions, such as assisting in protein folding (7), inhibiting protein aggregation (10), causing the disaggregation of aberrant protein oligomers (6), and facilitating the degradation of misfolded proteins (11).

In this study we have examined the effects of two intracellular and three extracellular chaperones on the toxicity of extracellularly added oligomers formed by three different peptides/proteins, namely the 42-residue amyloid β peptide (Aβ$_{42}$), the islet amyloid polypeptide (IAPP) and the N-terminal domain of the HypF protein from *E. coli* (HypF-N). We focused our attention on small oligomers as such species are generally highly toxic to cultured cells and are thought to be the major deleterious species in a range of protein aggregation diseases (4). We show that the chaperones markedly decrease the toxicity of preformed oligomers, with significant effects being observed even at molar ratios of protein:chaperone as high as 500:1. We show in addition that chaperones bind to the oligomers and promote their clustering into larger aggregates, in the absence of any disaggregation or major structural reorganisation. Overall, these results provide suggestions on novel mechanisms by which molecular chaperones are cytoprotective extracellularly and also

reveal new determinants of protein oligomer toxicity and strategies to convert protein aggregates that are toxic to cultured cells into innocuous species.

RESULTS

Chaperones reduce oligomer toxicity.

We generated toxic oligomers from $A\beta_{42}$, IAPP and HypF-N, as described previously (12-14). After 1 h incubation in the cell culture medium, they were added to human SH-SY5Y neuroblastoma cultured cells, at a corresponding monomer concentration of 12 µM. Under these conditions, all oligomers were found to decrease the MTT reduction of the cells by 30-40%, demonstrating their toxic nature (Fig. 1*A*). The oligomers were then subjected to the same procedure but incubated for 1 h in the cell culture medium containing either αB-crystallin (αBcr), Hsp70, clusterin (Clu), haptoglobin (Hp) or α_2-macroglobulin (α_2M) before their addition to SH-SY5Y cells. For these five chaperones and for all our experiments, the protein:chaperone molar ratios were 5:1, 5:1, 10:1, 15.1 and 100:1, respectively, unless otherwise stated. In each case the cells were found to reduce MTT to levels similar to untreated cells and to cells treated with the native proteins (Fig 1*A*). Hsp70 was found to be equally effective with or without ATP (SI Appendix. Fig. S1).

When the oligomers were incubated in the cell culture medium with proteins that do not act as chaperones, either hen lysozyme (HEWL) or bovine serum albumin (BSA), they maintained their toxicity (Fig. 1*A*). Moreover, chaperones were not found to be protective against other forms of stress, such as H_2O_2-mediated oxidation (SI Appendix. Fig. S2). These results therefore indicate that all five chaperones markedly decrease the toxicity of oligomers formed by three different proteins, with these effects being specific to the chaperones (relative to other proteins) and to protein oligomer toxicity (relative to other forms of stress).

The experiments with HypF-N oligomers and chaperones were repeated by varying the concentrations of each of the five chaperones (from 2.4 µM to 6 nm), while maintaining constant

4

that of HypF-N (12 µM). All chaperones had significant effects even at HypF-N:chaperone molar ratios of 500:1, becoming ineffective only at molar ratios of 2000:1 (Fig. 1*B*). Thus, chaperones appear to markedly decrease oligomer toxicity at greatly sub-stoichiometric concentrations. The experiments were repeated with HypF-N, Aβ_{42} and IAPP oligomers (12 µM) using varying concentrations of antibodies sequence-specific to the proteins (from 2.4 µM to 6 nm). Compared to the chaperones, higher concentrations of antibodies were required to reduce the toxicity of the respective oligomers (SI Appendix. Fig. S3).

Chaperones prevent the interaction of oligomers with cellular membranes.

For the following experiments we chose to focus on the oligomers from a single protein, HypF-N. Indeed, under different experimental conditions, HypF-N can aggregate into toxic (type A, the same used in the present work) or nontoxic (type B) oligomers; the two species are morphologically similar as determined by atomic force microscopy (AFM) and bind Thioflavin T (ThT) to similar levels, making it possible to carry out valuable control experiments (14). In addition, differences in the structure of toxic and nontoxic oligomers have been detected using the fluorescent probe *N*-(1-pyrene)maleimide (PM) (14), providing a valuable method to probe structural changes experienced by the oligomers following their exposure to chaperones (see below).

HypF-N oligomers have been shown to be toxic via aberrant interactions with the cell membrane, causing a rapid influx of Ca^{2+} ions from the cell culture medium to the cytosol (15). This triggers a slower and complex cellular cascade manifested by increases in intracellular ROS and in caspase-3 activity, and as a release of intracellular calcein from cells, eventually leading to apoptosis (15). Pre-incubation of HypF-N oligomers (12 µM monomer) with each of the five chaperones in the cell culture medium for 1 h, prior to addition to the cells, was found to inhibit the increase of intracellular Ca^{2+} levels caused by the oligomers (Fig. 2), with the degree of inhibition increasing with pre-incubation time (SI Appendix. Fig. S4). All other events were also reduced markedly, with the extent of reduction again being dependent on the time of pre-incubation (SI

5

Appendix. Fig. S5-7). We conclude, therefore, that all five chaperones examined here can inhibit the initial biochemical events induced by toxic HypF-N oligomers, namely the influx of Ca^{2+}, thus eliminating the occurrence of later downstream effects. In addition, the observed dependence of the degree of protection on the pre-incubation time indicates that the chaperones generically reduce toxicity by interacting with the oligomers, rather than through a separate protective pathway mediated by interaction of the chaperones with the cells.

Extracellular chaperones can interact with misfolded proteins and are thought to facilitate their clearance via endocytosis mediated by cell surface receptors, such as the lipoprotein receptor-related proteins 1 and 2 (LRP-1 and LRP-2) or scavenger receptors (9). This possibility was however excluded in our system, as shown by confocal microscopy and anti-HypF-N antibodies (SI Appendix. Fig. S8-9). In fact, HypF-N oligomers, unlike the native protein and nontoxic oligomers, were found to be internalised following pre-incubation for 1 h in the absence of chaperones. Analysis of the confocal images at median planes parallel to the coverslip revealed that HypF-N appeared inside the cells only upon treatment with the toxic oligomers. (SI Appendix. Fig. S8*B*). Pre-incubation of the oligomers with each chaperone led to little or no HypF-N entry (SI Appendix. Fig. S8-9). The oligomers were predominantly detected outside or attached to the cells, but not within them, as confirmed by analysing the confocal images at median planes. These observations therefore show that the chaperones inhibit oligomer internalisation, at least under the conditions used here, rather than stimulating their intracellular degradation following endocytosis.

We next took advantage of human embryonic kidney 293 (HEK293) cell lines overexpressing either human Hsp70 (HSPA1A) or Hsp22 (HSPB8) in the cytosol (16,17); the latter is a small heat shock protein containing an α-crystallin domain. Both cell lines were found to be resistant to intracellular protein aggregation-associated cell death (SI Appendix. Fig. S10) (16,17). As observed with the SH-SY5Y cells, treatment of wild-type HEK293 cells with HypF-N oligomers caused a decreased MTT reduction by 41±8%, whereas pre-incubation of the oligomers with either Hsp70 or αBcr prevented such an effect (SI Appendix. Fig. S10). Importantly, the HypF-N oligomers were

also toxic to HEK293 cells overexpressing Hsp70 or Hsp22, but pre-incubation of the oligomers with Hsp70 or αBcr prevented their toxicity in the corresponding cell lines (SI Appendix. Fig. S10).

Overall, therefore, the deleterious effects of HypF-N oligomers can be abolished by chaperones provided that the chaperone-oligomer interactions occur before the oligomers are able to interact with the cell membranes and initiate the Ca^{2+} influx. In agreement with this conclusion, chaperones overexpressed intracellularly are not protective against extracellular oligomers.

Chaperones bind to and assemble the oligomers into larger species.

Three possible non-exclusive molecular mechanisms can be hypothesised to explain how chaperones reduce oligomer toxicity: (i) the chaperones disassemble the oligomers; (ii) they bind to oligomers and promote their assembly into larger and innocuous aggregates, (iii) they catalyse a structural reorganisation into nontoxic forms. The ability of HypF-N oligomers to bind ThT was maintained following pre-incubation with each of the chaperones, whereas neither native HypF-N nor free chaperones had such an ability (SI Appendix. Fig. S11). A process of chaperone-mediated oligomer disassembly can thus be excluded.

To investigate whether chaperones bind to the oligomers and promote their further assembly, we first used AFM. Discrete oligomers with a height of 2-6 nm were observed by AFM in the absence of chaperones (Fig. 3*A*), but significantly larger aggregates are evident with αBcr (Fig. 3*B*) or $α_2$M (Fig. 3*C*), used here as representative chaperones. On higher magnification of these images, the aggregates appear as clusters of oligomers (Fig. 3*D*). In some cases more complex structures are observed, consisting of very large aggregates of irregular shape with typical heights of a few tens of nm, often surrounded by clusters of more distinct oligomers. Large assemblies are not observed in samples containing only chaperones (Fig. 3*E*,*F*).

The AFM data show that chaperones promote the assembly of the oligomers into larger species, but do not provide information on whether or not the chaperones remain bound to them. The oligomers can also be observed with confocal microscopy as, unlike free chaperones, they readily

7

adhere to the glass coverslips (Fig. 3*G*). Images obtained using oligomers pre-incubated with αBcr or α$_2$M show larger aggregates and co-localisation of the chaperones with the large oligomer clusters (Fig. 3*H,I*). Although this technique has a resolution that enables only visualisation of clusters of oligomers or areas enriched with oligomers (not individual oligomers), it shows that the chaperones are bound to the large clusters of oligomers.

In another experiment, samples of HypF-N oligomers incubated with each chaperone were centrifuged to separate the soluble (supernatant, SN) and insoluble (pellet, P) fractions, which were then analysed by SDS-PAGE. In the control samples containing oligomers or αBcr alone, the HypF-N monomer (MW ~10.5 kDa) and the αBcr monomer (MW ~20 kDa) bands were found only in the P and SN fractions, respectively (Fig. 4*A*). In the sample containing both species, the HypF-N band was found only in the P fraction, whereas αBcr was found to partition between the P and SN fractions (Fig. 4*A*). This finding indicates that a fraction of αBcr is bound to the oligomers. Moreover, the αBcr found in the P fraction remains tightly associated with the oligomers after resuspension of the pellet and further incubation (SI Appendix. Fig. S15). Similar results were obtained using α$_2$M (Fig. 4*B*), Hsp70 (SI Appendix. Fig. S12*A*), Clu (SI Appendix. Fig. S13*A*) and Hp (SI Appendix. Fig. S14*A*). The results, therefore, confirm that binding occurs between the oligomers and all five chaperones studied here. Intrinsic fluorescence spectra of the SN fractions collected in each experiment were also acquired (Fig. 4*C*, 4*D* and SI Appendix. Fig. S12*B*, S13*B*, S14*B*). The SNs obtained from the samples where both oligomers and chaperones were present yielded fluorescence spectra that were less intense than the corresponding samples in which only the chaperone was present, confirming that a fraction of the chaperone population had been separated through centrifugation.

Overall, the AFM data indicate that chaperones promote the assembly of the oligomers into larger species, whereas the other methods of analysis indicate that the chaperones are bound to the assembled oligomers. The finding that a small fraction of chaperones is bound to the oligomers, prompted by SDS-PAGE and intrinsic fluorescence measurements, suggests that chaperones act as

nucleation sites for the assembly of oligomers into larger species and explains why they are effective in reducing markedly oligomer toxicity even at highly sub-stoichiometric concentrations.

The molecular structure of the oligomers is preserved after chaperone interaction.

As a next step we set out to assess if chaperones promote a structural reorganisation of the oligomers, in addition to inducing their assembly. We took advantage of the ability to discriminate between the toxic HypF-N oligomers used in this work (type A) and nontoxic ones (type B) through the measurement of the fluorescence properties of oligomers labelled with PM at different positions in the sequence (14). This probe monitors the presence of a short distance (≤ 10Å) between labelled positions in the oligomers, which becomes evident as an excimer band at 440 nm (14). In particular, the fluorescence spectra of nontoxic oligomers formed by HypF-N labelled with PM at position 25, 55 or 87 show an excimer band at 440 nm that is very weak in the corresponding spectra obtained with PM-labelled toxic oligomers (Fig. 5*A*) (14). The fluorescence spectra obtained for the toxic oligomers labelled at each position after incubation with or without αBcr or α$_2$M are very similar and all show the absence of an excimer band (Fig. 5*A*), excluding a structural conversion. Similar data were obtained with Hsp70, Clu and Hp (SI Appendix. Fig. S12*C*, 13*C*, 14*C*).

We extended our analysis to oligomers formed from 1:1 mixtures of HypF-N monomers labelled with PM at 5 different positions (residues 10, 25, 47, 55, 87), thereby obtaining excimer ratio values for a total of 15 differently labelled HypF-N oligomers. The patterns of 15 excimer ratio values obtained in the presence of αBcr or α$_2$M, used as representative chaperones, are essentially identical to the pattern obtained in their absence (Fig. 5*B*), indicating that the spatial distribution of residues in the oligomers is preserved following interaction with the chaperones.

Furthermore, examination with Fourier transform infra-red (FTIR) spectroscopy indicated that no changes in secondary structure appeared to have occurred following the incubation of the oligomers with either αBcr or α$_2$M (Fig. 5*C*).

Discussion

Our data show that chaperones inhibit the cellular toxicity of extracellular protein oligomers under the conditions studied here. This behaviour appears to result from the ability of the chaperones to bind to oligomers and promote their further assembly into larger species, in the absence of any significant reorganisation of their internal molecular structure. This mechanism is extremely effective as it allows the chaperones to reduce oligomer toxicity at highly sub-stoichiometric levels.

Such an ability of molecular chaperones adds to their well established functions in facilitating protein folding, inhibiting protein aggregation and promoting the disaggregation and clearance of protein aggregates (6,7,10,11). In all our experiments the oligomers are formed before adding the chaperones, showing that the protective action of the latter also includes neutralisation of toxic oligomers after they have formed. This protective mechanism is not entirely novel, but evidence has been very sparse in the past, with reports often being contradictory and with undefined mechanisms (9,18-22).

These data also suggest that the size of extracellular protein aggregates is an inverse correlate of their toxicity. The chaperone-induced oligomer clusters are characterised by a reduction in their exposed hydrophobic surface and diffusional mobility, both of which are expected to reduce their toxicity to cells. It is therefore clear that chaperones can be valuable tools for understanding the factors governing oligomer toxicity.

Importantly, the results shown here suggest that the structure, function and mechanism of action of molecular chaperones may serve to guide the design of therapeutic interventions against diseases originating from extracellular protein aggregation. Indeed, the finding that natural molecular chaperones can inhibit the toxicity of aberrant protein aggregates after they are formed, with broad specificity and at very low concentrations, suggests that therapeutics based on the same type of intervention could be effective against such diseases.

Materials and methods

Proteins

HypF-N was purified as previously described (14). $A\beta_{42}$ and IAPP were purchased from Sigma-Aldrich (St. Louis, MO). Human Hsp70 and αBcr were purified as previously described (23,24). Human Clu, α_2M and Hp were purified as previously reported (25-27). BSA and HEWL were obtained from Sigma-Aldrich.

Formation of protein oligomers

HypF-N was converted into toxic (type A) or nontoxic (type B) aggregates as previously reported (14). Oligomers were centrifuged at 16100g for 10 min, dried under N_2 and resuspended in the cell culture medium without cells (for cell biology tests) or in 20 mM phosphate buffer, pH 7.0 (for biophysical/biochemical analysis). No significant dissolution of the oligomers or change in morphology/structure could be detected after this procedure, as previously reported (14). Toxicity was measured in all cases under physiological conditions (pH 7.4, 37 °C, no organic solvents). $A\beta_{42}$ and IAPP oligomers were prepared as previously described (12,13) and resuspended in the cell culture medium to 12 µM. Native proteins were diluted to 12 µM into the same medium. All oligomers were then incubated in the appropriate media for 1 h at 37 °C while shaking, without or with chaperones, and then added to cultured cells or subjected to biophysical/biochemical analysis. The HypF-N($A\beta_{42}$/IAPP):chaperone molar ratio was 5:1 (αBcr), 5:1 (Hsp70), 10:1 (Clu), 15:1 (Hp) and 100:1 (α_2M), unless stated otherwise (all proteins are considered as monomers, except Clu and Hp as αβ dimers and α_2M as a tetramer).

MTT reduction assay

Oligomers of HypF-N, Aβ$_{42}$ and IAPP (at a corresponding monomer concentration of 12 μM) were incubated for 1 h without or with αBcr, Hsp70, Clu, Hp, α$_2$M, HEWL or BSA (HypF-N:chaperone molar ratios as described above, HypF-N:HEWL and HypF-N:BSA molar ratios were 5:1), and then added to SH-SY5Y cells. The MTT reduction assay was performed as previously described (14). Further details are give in Supplementary Methods.

Measurement of intracellular Ca^{2+}

HypF-N oligomers (at a corresponding monomer concentration of 12 μM) were incubated for 1 h in the cell culture medium without or with αBcr, Hsp70, Clu, Hp or α$_2$M and then added to SH-SY5Y cells seeded on glass coverslips for 60 min at 37 °C. Cells were then loaded with 10 μM fluo3-AM (Molecular Probes, Eugene, OR), as previously described (14,15). Cells were also treated with nontoxic HypF-N oligomers or the native protein (12 μM monomer). Cell fluorescence was analysed by confocal scanning microscopy, as previously described (14,15).

AFM

Samples prepared as detailed above were diluted from 5 to 100 times, as required, and 10 μl aliquots were deposited on freshly cleaved mica and dried under mild vacuum. Tapping mode AFM images were acquired in air using a Multimode SPM, equipped with a "E" scanning head (maximum scan size 10μm) and driven by a Nanoscope IV controller, and a Dimension 3100 SPM, equipped with a 'G' scanning head (maximum scan size 100μm) and driven by a Nanoscope IIIa controller (Digital Instruments, Bruker AXS GmbH, Karlsruhe, Germany). Single beam uncoated silicon cantilevers (type OMCL-AC160TS, Olympus, Tokyo, Japan) were used. The drive frequency was 290-310 kHz, the scan rate was 0.4-0.8 Hz. Aggregate sizes were measured from the height in cross section of the topographic AFM images. The reported heights result from the

obtained values multiplied by a shrinking factor of 2.2, which was evaluated comparing the heights of native HypF-N under liquid and after drying.

Confocal microscopy analysis for chaperone-oligomer binding

HypF-N oligomers (at a corresponding monomer concentration of 48 μM) were incubated for 1 h without or with αBcr or α_2M and then centrifuged to obtain pellets which were resuspended and incubated subsequently for 30 min at 37 °C in solutions containing: (i) 1:4000 rabbit polyclonal anti-HypF-N antibodies (Primm, Milan, Italy) and goat polyclonal anti-αBcr antibodies or goat polyclonal anti-α_2M antibodies (Santa Cruz Biotech, Santa Cruz, CA); (ii) 1:1000 Alexa Fluor 488-conjugated anti-rabbit secondary antibodies (Molecular Probes); (iii) 1:4000 Texas red-conjugated anti-goat secondary antibodies (Santa Cruz Biotech). After every incubation, samples were centrifuged for 10 min at 16100g, washed in PBS and centrifuged again. Finally, the P was resuspended in 20 μl PBS and spotted on glass coverslips. The cross-reactivity of oligomers was tested by subsequent incubations with primary and secondary anti-αBcr or anti-α2M antibodies. Confocal microscope images were acquired as previously described (14).

SDS-PAGE

HypF-N oligomers, αBcr and α_2M were incubated for 1 h in 20 mM phosphate buffer at pH 7.0 in isolation and in combination (48 μM HypF-N). Samples were then centrifuged for 10 min at 16100g. Aliquots of the P and SN fractions were subjected to SDS-PAGE using 15% polyacrylamide gels.

Intrinsic fluorescence

Intrinsic fluorescence spectra of the SN fractions collected for SDS-PAGE were acquired at 37 °C using a Perkin-Elmer LS 55 spectrofluorimeter (Wellesley, Massachusetts) and a 2X10mm quartz cell, an excitation wavelength of 280 nm. The spectrum of HypF-N oligomers was subtracted from

that of the chaperone in the presence of HypF-N oligomers and all the spectra were normalized to the maximum fluorescence intensity of the chaperone spectrum.

Pyrene fluorescence

HypF-N variants carrying a single cysteine residue were labelled with PM as previously described (14), converted into toxic and nontoxic oligomers in homogeneous or 1:1 mixtures and then diluted 4-fold into 20 mM phosphate buffer at pH 7.0. Fluorescence emission spectra of these samples were acquired after 1 h without or with chaperones and analyzed as previously described (14). HypF-N concentration was 12 μM.

FTIR spectroscopy

HypF-N oligomers were incubated with or without αBcr or α$_2$M (48 μM HypF-N) and then centrifuged and resuspended in D$_2$O twice to achieve a final protein concentration of ~15 mg ml^{-1}. The sample was deposited on a KBr window in a semipermanent liquid cell and the FTIR spectra were recorded at room temperature using an FT/IR 4200 spectrophotometer (Jasco, Tokyo, Japan). The system was constantly purged with N$_2$. The resulting spectra were baseline corrected and smoothed.

Statistical analysis

All data were expressed as means ± standard deviation (SD). Comparisons were performed using ANOVA followed by Bonferroni's post-comparison test.

Author contributions

B.M., R.C., C.C. and F.C. designed the experiments and interpreted the data. B.M. and R.C. performed the experiments with the contributions from M.Z., M.v.W., S.C. and M.B. S.M., C.R. and M.R.W. provided the molecular chaperones. A.P. and A.R. designed, performed and analyzed the AFM experiments. C.C. supervised the experiments on cell cultures. F.C. supervised all the experiments. B.M., R.C., C.M.D., M.R.W. and F.C. wrote the manuscript with contributions from A.R., C.R., H.K. and C.C.

References

1. Monsellier E, Chiti F (2007) Prevention of amyloid-like aggregation as a driving force of protein evolution. *EMBO Rep* 8:737-742.

2. Powers ET, Morimoto RI, Dillin A, Kelly JW, Balch WE (2009) Biological and chemical approaches to diseases of proteostasis deficiency. *Annu Rev Biochem* 78:959-991.

3. Selkoe DJ (2003) Folding proteins in fatal ways. *Nature* 426:900-904.

4. Chiti F, Dobson CM (2006) Protein misfolding, functional amyloid, and human disease. *Annu Rev Biochem* 75:333-366.

5. Morimoto RI (2008) Proteotoxic stress and inducible chaperone networks in neurodegenerative disease and aging. *Genes Dev* 22:1427-1438.

6. Weibezahn J, Schlieker C, Tessarz P, Mogk A, Bukau B (2005) Novel insights into the mechanism of chaperone-assisted protein disaggregation. *Biol Chem* 386:739-744.

7. Hartl FU, Bracher A, Hayer-Hartl M (2011) Molecular chaperones in protein folding and proteostasis. *Nature* 475:324-332.

8. Bukau B, Weissman J, Horwich A (2006) Molecular chaperones and protein quality control. *Cell* 125:443-451.

9. Wilson MR, Yerbury JJ, Poon S (2008) Potential roles of abundant extracellular chaperones in the control of amyloid formation and toxicity. *Mol Biosyst* 4:42-52.

10. Broadley SA, Hartl FU (2009) The role of molecular chaperones in human misfolding diseases. *FEBS Lett* 583:2647-2653.

11. Pickart CM and Cohen RE (2004) Proteasomes and their kin: proteases in the machine age. *Nat Rev Mol Cell Biol* 5:177-187

12. Lambert MP, *et al*. (2001) Vaccination with soluble Aβ oligomers generates toxicity-neutralizing antibodies. *J Neurochem* 79:595-605.

13. Cecchi C, *et al*. (2008) Replicating neuroblastoma cells in different cell cycle phases display different vulnerability to amyloid toxicity. *J Mol Med* 86:197-209.

14. Campioni S, *et al*. (2010) A causative link between the structure of aberrant protein oligomers and their toxicity. *Nat Chem Biol* 6:140-147.

15. Zampagni M, *et al*. (2011) A comparison of the biochemical modifications caused by toxic and nontoxic protein oligomers in cells. *J Cell Mol Med* 15:2106-2116.

16. Nollen EA, Brunsting JF, Roelofsen H, Weber LA, Kampinga HH (1999) *In vivo* chaperone activity of heat shock protein 70 and thermotolerance. *Mol Cell Biol*. 19:2069-2079.

17. Carra S, *et al*. (2010) Identification of the Drosophila ortholog of HSPB8: implication of HSPB8 loss of function in protein folding diseases. *J Biol Chem* 285:37811-37822.

18. Fabrizi C, Businaro R, Lauro GM, Fumagalli L (2001) Role of α2-macroglobulin in regulating amyloid β-protein neurotoxicity: protective or detrimental factor? *J Neurochem* 78:406-412.

19. Oda T, *et al*. (1995) Clusterin (apoJ) alters the aggregation of amyloid β-peptide (Aβ$_{1-42}$) and forms slowly sedimenting Aβ complexes that cause oxidative stress. *Exp Neurol* 136:22-31.

20. Boggs LN, *et al*. (1996) Clusterin (ApoJ) protects against *in vitro* amyloid-β (1-40) neurotoxicity. *J Neurochem* 67:1324-1327.

21. Du Y, *et al*. (1998) α2-macroglobulin attenuates β-amyloid peptide 1-40 fibril formation and associated neurotoxicity of cultured fetal rat cortical neurons. *J Neurochem* 70:1182-1188.

22. Yerbury JJ, *et al*. (2007) The extracellular chaperone clusterin influences amyloid formation and toxicity by interacting with prefibrillar structures. *FASEB J* 21:2312-2322.

23. Roodveldt C, *et al*. (2009) Chaperone proteostasis in Parkinson's disease: stabilization of the Hsp70/α-synuclein complex by Hip. *EMBO J* 28:3758-3770.

24. Waudby CA, *et al*. (2010) The interaction of αB-crystallin with mature α-synuclein amyloid fibrils inhibits their elongation. *Biophys J* 98:843-851.

25. Wilson MR, Easterbrook-Smith SB (1992) Clusterin binds by a multivalent mechanism to the Fc and Fab regions of IgG. *Biochim Biophys Acta* 1159:319-326.

26. French K, Yerbury JJ, Wilson MR (2008) Protease activation of α2-macroglobulin modulates a chaperone-like action with broad specificity. *Biochemistry* 47:1176-1185.

27. Yerbury JJ, Rybchyn M, Easterbrook-Smith SB, Henriques C, Wilson MR (2005) The acute phase protein haptoglobin is a mammalian extracellular chaperone with an action similar to clusterin. *Biochemistry* 44:10914-10925.

Figure Legends

Fig. 1. Reduction of protein oligomer toxicity by chaperones. (*A*) Preformed oligomers of HypF-N, $A\beta_{42}$ and IAPP were resuspended in the cell culture medium at a corresponding monomer concentration of 12 μM, incubated for 1 h without or with the indicated chaperones or control proteins, and then added to the cell culture medium of SH-SY5Y cells. The asterisks indicate $p \leq 0.01$ relative to the experiment without chaperones. (*B*) Similarly treated HypF-N oligomers (12 μM monomer) were incubated for 1 h without (O) or with the indicated chaperones at the indicated HypF-N:chaperone molar ratios, and then added to SH-SY5Y cells. The scale on the *x* axis is logarithmic.

Fig. 2. Reduction of HypF-N oligomer-induced intracellular free Ca^{2+} influx by chaperones. Confocal microscope images of SH-SY5Y cells showing intracellular free Ca^{2+} following exposure to HypF-N oligomers (at a corresponding monomer concentration of 12 μM) pre-incubated with or without the indicated chaperones. The green fluorescence arises from the intracellular Fluo3 probe bound to Ca^{2+}.

Fig. 3. Assembly of HypF-N oligomers induced by chaperones. (*A-F*) AFM images (left, height data; right, amplitude data) showing oligomers and chaperones pre-incubated in phosphate buffer alone or in combination, as indicated; scan size, 630 nm. (*D*) Enlargement of a 250x250 nm portion of (*B*). Z range: 10 nm (*A*), 13 nm (*B,D*), 25 nm (*C*), 6 nm (*E*), 10 nm (*F*). (*G*) Representative confocal microscope images showing HypF-N oligomers without chaperones and treated with anti-α_2M (red), anti-αBcr (red) or anti-HypF-N (green) antibodies, as indicated. The absence of red fluorescence indicates the absence of cross-reaction. (*H,I*) Images showing HypF-N oligomers

incubated with αBcr (*H*) or α$_2$M (*I*) and treated with the same three antibodies, as indicated. The co-localization of oligomers and chaperones is shown in the merged images (yellow).

Fig. 4. Binding of chaperones to HypF-N oligomers. (*A*) SDS-PAGE analysis of the P and SN fractions of samples containing HypF-N oligomers (lanes 2,3), αBcr (lanes 4,5) and oligomers with αBcr (lanes 6,7). The bands at ~10 and 20 kDa indicate monomeric HypF-N and αBcr, respectively. The HypF-N concentration was 48 µM. (*B*) SDS-PAGE analysis for α$_2$M; conditions and lanes as in (*A*). The α$_2$M bands range from ~ 60 kDa to ~ 160 kDa. (*C*) Intrinsic fluorescence spectra of the SN fractions of samples containing HypF-N oligomers (dotted line), αBcr (solid line) and oligomers with αBcr (dashed line). The spectrum of HypF-N oligomers has been subtracted from that of chaperone plus oligomers to clear the contribution of the former. All spectra are the means of three experiments. (*D*) Intrinsic fluorescence analysis of α$_2$M. Conditions and spectra as in (*C*).

Fig. 5. Lack of structural reorganization of HypF-N oligomers following treatment with chaperones. (*A*) Fluorescence emission spectra of HypF-N oligomers labelled with PM at positions 25 (top graphs), 55 (middle graphs) and 87 (bottom graphs). The HypF-N concentration was 12 µM. The spectra refer to oligomers incubated in 20 mM phosphate buffer, pH 7.0 without (black) and with αBcr (red) or α$_2$M (purple). For comparison, the corresponding spectra of nontoxic oligomers are reported in each graph (green). The spectra are normalized to the intensity of the peak centred at 375 nm. The vertical lines at 440 nm indicate the position of the excimer band. (*B*) Ratios between the PM fluorescence intensities measured at 440 nm (excimer peak) and 375 nm (PM monomer peak) for HypF-N oligomers prepared with 1:1 mixtures of HypF-N chains PM-labelled at positions 10, 25, 47, 55 and 87. Colours as in (A). The total HypF-N concentration was 12 µM. The SD are reported in brackets. (*C*) FTIR amide I spectra of HypF-N oligomers after incubation without (black) and with αBcr (red) or α$_2$M (purple).
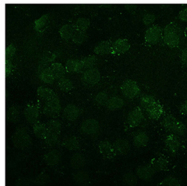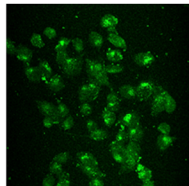
A
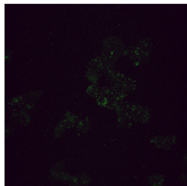
B
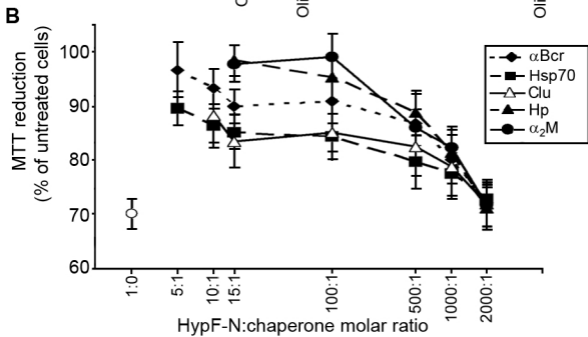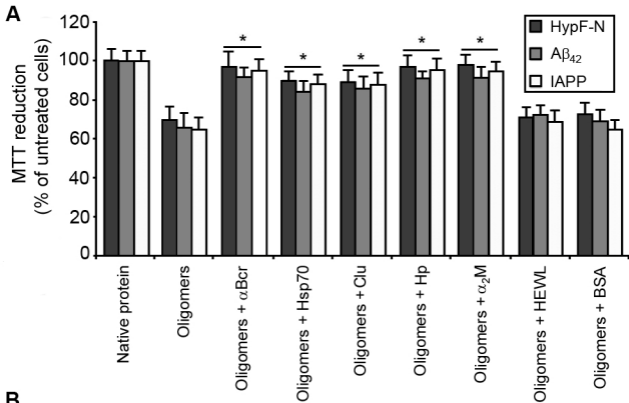
Analysis of Ca²⁺ influx
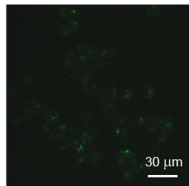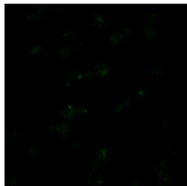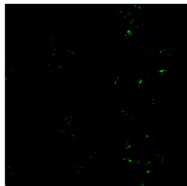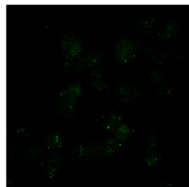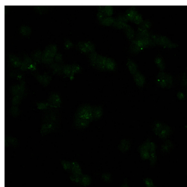
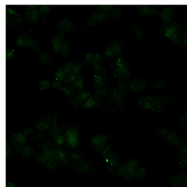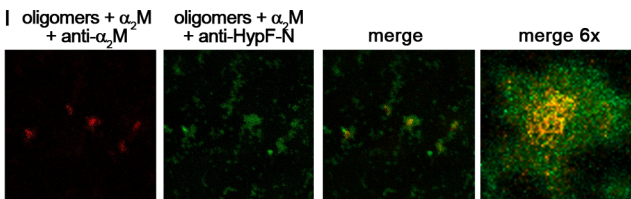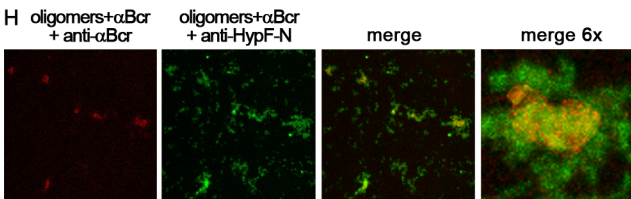|		
Untreated cells	Native HypF-N	Nontoxic oligomers
Oligomers	Oligomers + αBcr	Oligomers + Hsp70
Oligomers + Clu	Oligomers + Hp	Oligomers + α₂M

30 μm

A   oligomers

B   oligomers + αBcr

C   oligomers + α₂M

D   oligomers + αBcr

E   α₂M

F   αBcr

G   oligomers + anti-α₂M   oligomers + anti-αBcr   oligomers + anti-HypF-N   oligomers + anti-HypF-N 6x

30 μm   5 μm

H   oligomers+αBcr + anti-αBcr   oligomers+αBcr + anti-HypF-N   merge   merge 6x

I   oligomers + α₂M + anti-α₂M   oligomers + α₂M + anti-HypF-N   merge   merge 6x

A

	P	SN	P	SN	P	SN
oligomers	+	+	−	−	+	+
αBcr	−	−	+	+	+	+

24
20.1
14.2
6.5

B

	P	SN	P	SN	P	SN
oligomers	+	+	−	−	+	+
α_2M	−	−	+	+	+	+

205
97.4
55
14.2
6.5

C

intrinsic fluorescence (a.u.)

αBcr

αBcr + oligomers

oligomers

wavelength (nm)

D

intrinsic fluorescence (a.u.)

α_2M

α_2M + oligomers

oligomers

wavelength (nm)

A

Labeled residue: 25 (left panel)
- oligomers (black)
- oligomers + αBcr (red)
- nontoxic oligomers (green)

Labeled residue: 25 (right panel)
- oligomers (black)
- oligomers + α$_2$M (purple)
- nontoxic oligomers (green)

Labeled residue: 55

Labeled residue: 55

Labeled residue: 87

Labeled residue: 87

Y-axis: normalised PM fluorescence intensity
X-axis: wavelength (nm)

B

	10	25	47	55	87
10	0.14 (.002) 0.13 (.009) 0.14 (.004)				
25	0.18 (.016) 0.18 (.010) 0.21 (.012)	0.32 (.054) 0.29 (.012) 0.32 (.012)			
47	0.18 (.019) 0.12 (.010) 0.12 (.001)	0.14 (.045) 0.15 (.026) 0.15 (.028)	0.09 (.017) 0.11 (.003) 0.11 (.003)		
55	0.14 (.012) 0.17 (.008) 0.18 (.004)	0.24 (.005) 0.23 (.008) 0.28 (.065)	0.12 (.031) 0.14 (.009) 0.14 (.013)	0.22 (.025) 0.22 (.015) 0.22 (013)	
87	0.14 (.014) 0.14 (.019) 0.15 (.007)	0.22 (.022) 0.22 (.034) 0.23 (.011)	0.09 (.022) 0.12 (.02) 0.13 (.005)	0.18 (.002) 0.17 (.001) 0.15 (.003)	0.19 (.032) 0.29 (.022) 0.16 (.014)

C

- oligomers (black)
- oligomers + αBcr (red)
- oligomers + α$_2$M (purple)

Y-axis: absorbance
X-axis: wavenumber (cm^{-1})